ADVANCES IN MATERIALS SCIENCE, Vol. 22, No. 3 (73), September 2022

DOI: 10.2478/adms-2022-0010

Mehmet Kul[1], Yasin Yılmaz[2*], Kürşad Oğuz Oskay[3], Levent Cenk Kumruoğlu[4]

[1] Department of Metallurgical and Materials Engineering, Sivas University of Science and Technology, 58000, Sivas, Turkey
[2] Department of Aeronautical Engineering, Sivas University of Science and Technology, 58000, Sivas, Turkey
[3] Department of Metallurgical and Materials Engineering, Sivas Cumhuriyet University, 58000, Sivas, Turkey
[4] Department of Metallurgical and Materials Engineering, İskenderun Technical University, 31200, İskenderun, Turkey

***** yyilmaz@sivas.edu.tr

EFFECT OF CHEMICAL COMPOSITION OF BORIDING AGENT ON THE OPTIMIZATION OF SURFACE HARDNESS AND LAYER THICKNESS ON AISI 8620 STEEL BY SOLID AND LIQUID BORIDING PROCESSES

ABSTRACT

Surfaces of cam shafts made of AISI 8620 steels were hardened by boriding processes in both solid and liquid mediums. Various chemical agents were used to achieve boride layers on the surfaces of the cam shafts in these processes. It was aimed to examine effects of the chemical agents on microhardness and thickness of the boride layers obtained. It was concluded that a bath composition of 5% B_4C-90% SiC-5% KBF_4 was appropriate for the hardest and thickest boride layer achieved in the solid medium, and a composition of 70% $Na_2B_4O_7$-30% B_4C in the liquid medium.

Keywords: *Solid and liquid boriding; iron borides; diffusion; optimization; surface characteristic*

INTRODUCTİON

AISI 8620 is a kind of carbon steel mainly used in lubricated sliding components such as gears and camshafts [1]. Such components are often damaged catastrophically without any warning because of the sliding wear [2–4]. Therefore, they must be replaced with new ones after a certain period of time. However, this causes a serious loss of money, time and material. To minimize these problems, it is important that such materials must have improved surface properties such as friction and wear resistance [5,6]. This has led to development of various surface treatments [7–10]. Therefore, a number of surface treatments have been developed for such materials to improve surface microhardness and corrosion and the wear resistance. Such surface treatments include physical vapor deposition (PVD), chemical vapor deposition (CVD), electrochemical deposition, spray deposition, and thermochemical diffusion processes. By means of these methods, it is aimed to improve the surface properties of metals

and alloys by depositing carbide, nitride and boride layers that are resistant to the wear, the corrosion and oxidation [11,12]. Boriding is one of the surface treatments because the boride layers achieved are strongly adhered to the metals and the alloys through the thermochemical diffusion processes [8,9]. The process encompasses thermo-diffusion of individual boron atoms into the surfaces of the alloys, followed by their chemical reaction with boron-forming agents present on their surfaces to form hard and durable boride layers [9]. This thermochemical diffusion process can be applied to numerous metals and alloys to achieve the hard, the corrosion and the wear resistant layers on them [13]. When compared to other thermochemical diffusion surface treatments such as carburising and nitriding processes, it can be mentioned that much better surface properties are obtained by the boriding process [14,15]. The boriding process of ferrous alloys usually requires 1 to 10 hours of the treatment at temperatures between 850 and 1000 °C [8,16]. By means of the diffusion of the boron atoms into the ferrous alloys, two different iron borides (FeB and Fe_2B) are formed in microstructure of the boride layers [17]. These boride layers can adhere strongly to the surface of the ferrous alloys due to saw-tooth morphology of the layers [18,19]. However, owing to nature of the boriding process, some disadvantages arise, especially with formation of the FeB layer, which are quite brittle [20]. The boriding process can be applied to all ferrous and non-ferrous metals and alloys [14,21] in solid, liquid and gas medium [22,23]. The the solid boriding process is most widely used due to its ease of process, simplicity of the equipment used in the process and not being economically expensive [24]. The agents such as boron carbide, amorphous boron and ferro-boron, alkaline metals, ammonium boron fluorides, fillers or non-reactive agents such as KBF_4, AlF_3, NaCl, NH_4Cl, SiC and Al_2O_3 are mixed in certain proportions [25]. The liquid boriding is carried out by immersing the metallic alloys in a molten salt bath containing the agents. The most important benefits of the liquid boriding process are possibility of quenching to the alloy directly after the boriding process and energy savings due to no need to heat containers with powder mixture consisting of the agents compared to the solid boriding process [25]. For example, liquid borax baths as a reductant have been proposed by Allaoui et al. [26]. The agents and composition of boriding medium are highly competitive in the formation of the boride layers. There is an interest and literature basic for the boriding medium of the ferrous alloys [21,27]. Although there are several studies about the boriding process for the ferrous alloys in the literature, it has not been performed in the different mediums with variable chemical composition of the agents or even if there are, it is very limited. Thus, purpose of this work is to determine effect of the chemical composition of the agents and the mediums on the microhardness and the microstructure of achived boride layers. In this way, 15 different boriding compositions containing the different agents with the different content were utilized for the boriding processes of the AISI 8620 steels. Compared to other boriding compositions, it was seen that the chemical compositions used in the solid and the liquid boriding processes, where optimal microhardness and thickness of the boride layer obtained, are 5% B_4C-90% SiC-5% KBF_4 and 70% $Na_2B_4O_7$-30% B_4C respectively.

EXPERİMENTAL

Chemical composition of the AISI 8620 steel is found to be 0.18 wt. % C, 0.24 wt. % Si, 0.85 wt. % Mn, 0.02 wt. % P, 0.03 wt. % S, 0.55 wt. % Cr, 0.21 wt. % Mo, 0.50 wt. % Ni, and rest Fe by spectrometry and it is given in Table 1. The steels were emplaced in ceramic crucibles for the boriding processes in the solid (A1-A7) and the liquid (A8-A15) mediums in a Protherm lab type furnace at 950ºC for 4 h. According to Table 2, a 20 g mixed boriding agent as total was used for each boriding process. Thickness of the boride layers achieved

were measured with the aid of an optical microscope. The microhardness tests were performed by *Struers Duramin A300* static micro-indentation analysis using Vicker's microhardness device in depths of 30, 45, 60, 75 and 90 μm starting from the surface of the boride layers under an indentation load of 0.5 kg, and an average microhardness value for each depth out of at least five counts of repeated measurements was achieved. The steels with the boride layer were subjected to metallographic examination. For this, they were mounted in a resin and ground by means of 1200 grid SiC paper and polished by alumina suspension of 1 μm. After that, they were ethced by using Nital (HNO_3, 3% by volume) solution. Physical and chemical analysis of the steels were performed by *Carl Zeiss* optical microscopy (OM), a *FEI Quanta FEG 250* scanning electron microscopy (SEM), energy dispersive X-ray spectroscopy (EDX) and a *Bruker D8 Advance* X-ray diffraction (XRD) method with a CuKα radiation (λ Kα =1.54 Å).

Table 1. *Chemical composition of the AISI 8620 steel, wt.%*

C	Si	Mn	P	S	Cr	Mo	Ni	Fe
0.18	0.24	0.85	0.02	0.03	0.55	0.21	0.50	rest

RESULTS AND DİSCUSSİON

The solid boriding processes were performed in A1-A7 experiments as seen in the Table 2. Several agents were used here. The B_4C is essential boron providing agent as in ref. [27], so it was used in A1, A2, A3, A5, A6 and A7 experiments. The highest microhardness and the thickest and the most homogeneous boride layer was obtained in the A7 experiment according to in the Table 2 and Fig.1. Addition of the B_4C used together with the KBF_4 is essential for hard, thick and the homogeneous boride layer. At the boriding process temperature, BF_3 vapor is formed by the KBF_4 and this gas reacts with the boron-forming agent, the B_4C to provide the boriding medium. As a result, this medium reacts with the surface of the steel. Nucleation occurs on the surface of the steel when this medium interacts to its surface, hence, the thick, the hard and the homogeneous boride layer can be achieved [28]. As seen in the Table 2 and the Fig. 1, some of the compositions of the agents (A1-A4) commonly used in the literature are improper for the solid boriding process of the steel. It is seen that the boride layer do not form on the surface of the steel in the A1 experiment according to the Table 1 and the Fig. 1. The agents in this experiment showed only a thin boride layer adhering weakly to the surface of the steel. This means that existing composition here is improper for the solid boriding process of the steel. As known, Na_2CO_3 has a lower melting temperature like NaCl, NaOH, $CaCl_2$ hence it decreases viscosity of the boriding medium, therefore diffusing of the boron atom is expected to be easy and be thicker boride layer [21] however, this phenomenon didn't occur in this case. Similar case has been observed in the boriding process of AISI 1045 steel in both the solid and the liquid mediums containing different agents performed by Kul et. al [27]. The composition of the boriding medium containing B_4C, SiC and KBF_4 in the A6 experiment, formed a relatively thick boride layer, but FeB phase in the microstructure caused to spalling and cracking due to excessive residual stresses arised in the layer. This case on the A6 experiment mean that the boride layer consisting of more Fe_2B layer rather than the FeB layer have to be preferred, since the FeB layer is comparatively more brittle owing to its richer boron quantity than that of the Fe_2B layer. On the other hand, thermal expansion coefficient of the FeB layer is higher than that of the Fe_2B layer. Along with double boride layer consisting of more FeB and less Fe_2B exfoliating and cracks would form due to difference in these thermal expansion coefficients [19, 29]. Thus, according to ref. [27], it can

be mentioned that this problem can be overcomed by reducing the amount of the B_4C a as shown in the Table 2 and the Fig.1. As well known, some alloying elements such as C, Si etc. are insoluble in the boride layers and they are gathered in adjacent-to-borides thin interlayers. Therefore, these elements adjacent to base metal affect mechanism of the boriding process. As a result, the microstructure of the boride layer changes [30,31]. According to the Table 2 and the Fig.1, in the liquid boriding process, the highest microhardness of 1360 $HV_{0.5}$ and the thickest and uniform boride layer was achieved with A11 experiment using the agents such as the B_4C and the borax. In this experiment, an entire mixture of boron-rich composition, and positive effects of the agents may have could result in the forming of a thicker and harder boride layer as in ref. [21] and ref. [27], respectively. Also, in A13 experiment, the borax and the SiC agents showed homogeneous and adhearable boride layer to the steel likely due to a process of entire mixture of the agents in the ref. [21] and positive effect of them to the steel as in the ref. [27] as seen in the Fig. 1 and the Table 2. Yet, in this experiment, the boride layer with optimal microhardness and the thickness did not form. This can be explained by potential difference among the steel and the SiC that acts as microanodes and does not sufficient boron diffusion according to the ref. [27]. Considering the microhardnesses and the OM images given in the Table 2 and the Fig. 1, it can be mentioned that the Na_2CO_3, Fe-Si, B_2O_3, B_4C and SiC agents (used in the A8, the A11 and the A13 experiments) are preferable for the liquid boriding process of the steel. As stated before that in ref. [26], depending on Ellingham's diagrams, reduction of boron oxide arising from thermal disintegration of the borax is made simpler by aluminum than carbon or silicon. However, this case was not occured in this study as shown in the microhardness distribution of the A12 experiment in the Table 2. Also, a galvanic cell is needed for the boriding process by means of dissolved salts. For this, there must be an electrochemical difference and electrical contact between the metallic alloy and reducing agent. So that cathodic reaction take place on the surface of the alloy, electrode potential of the alloy must be positive under conditions such as electrolyte composition, the temperature and higher than that of the reducing agent. The electrode potential of the cathodic reaction on the surface of the alloy may be negative and/or lower than that of the reducing agent, therefore, no boride layer may have not could appear on the surface of the steel in the A15 experiment according to ref. [21]. Hence, it is seen that some of the agents showing promising results in the literature were not effective in the liquid boriding process as seen in the A12 and the A15 experiments.

Table 2. *The chemical composition of the boriding agents and the microhardness profiles of the boride layers at various depths from the surface (A1-A7: solid boriding experiments and A8- A15: liquid boriding experiments)*

Mixture	Composition, (wt. %)			Microhardness ($HV_{0.5}$) distances from the surface				
				30 μm	45 μm	60 μm	75 μm	90 μm
A1	B_4C, 85	Na_2CO_3, 15		183	177	156	145	101
A2	B_4C, 95	NaCl, 5		458	418	231	155	137
A3	B_4C, 95	Borax, 5		547	489	301	214	115
A4	SiC, 85	B_2O_3, 15		242	165	163	156	127
A5	B_4C, 85	NaOH, 15		978	968	760	303	236
A6	B_4C, 50	SiC, 45	KBF_4, 5	1213	700	263	220	172
A7	B_4C, 5	SiC, 90	KBF_4, 5	1348	1250	1131	986	391
A8	Borax, 65	Na_2CO_3,10	Fe-Si, 25	1281	1139	903	724	272
A9	Borax, 65	NaOH,10	Fe-Si, 25	1103	1062	810	342	166
A10	Borax, 65	B_2O_3, 10	Fe-Si, 25	1128	1106	885	638	245
A11	Borax, 70	B_4C, 30		1360	1299	1238	1179	1011
A12	Borax, 70	Al*, 30		259	151	144	132	117
A13	Borax, 70	SiC, 30		1320	1216	1058	981	748
A14	Borax, 65	Fe-Si, 25	$CaCl_2$, 10	1192	1137	704	439	-
A15	Borax, 73	SiC,24	NaCl, 3	321	457	215	-	-

The Fig. 1 shows the OM images of the steels with boride layer (The solid boriding experiments are the A1, the A3 and the A7 experiments, while the liquid boriding experiments are the A10, the A11, the A13, and the A15 experiments). Fig. 2 shows the scanning electron microscopy (SEM) images taken from the cross sections of the steels with the boride layer in the A11 and the A13 experiments. As can be seen, the boride layers showed saw-tooth morphology typical for the ferrous alloys as reported before [9,22,27,32]. The steel in the A11 experiment comprises two different boride layers i.e, both FeB and Fe_2B and data of the EDX analysis of regions of 1, 2 and 3 showed in Table 3 supports this situation, while the steel in the A13 experiment comprise a single boride i.e, Fe_2B respectively. Since desired single boride layer formation was obtained in the A13 experiment, chemical composition of this experiment is suitable. As said before above that the hardest and thickest boride layer was achieved in the steel in the A11 experiment, on the other hand, an undesirable double boride layer was formed with some FeB layer beside the Fe_2B layer here. This case was also confirmed by XRD pattern for each steel with the boride layer as illustrated in Fig. 3. Which layer is occured in the boriding process is determined by parameters such as the chemical composition of the metal to subject the boriding process, temperature-time, boron potential at the surface of the alloy, and the medium and processing method [22,26,28].

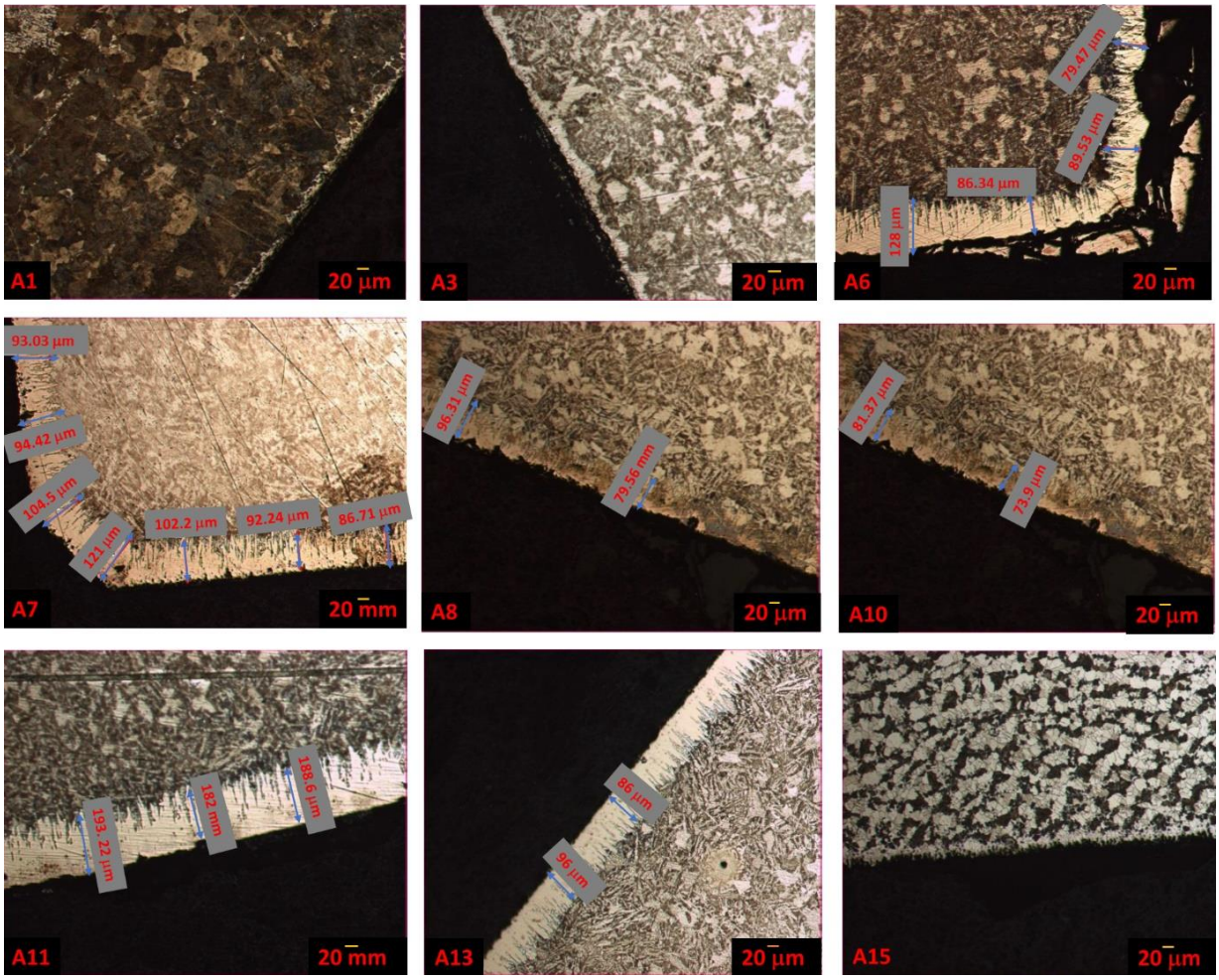


Fig. 1. OM images of the AISI 8620 steels with the boride layer (The solid boriding processes are the A1, the A3, the A6 and the A7 experiments, while the liquid boriding processes are the A10, the A11, the A13, and the A15 experiments)

Beside of these, as experimentally shown the microstructure of the boride layers depends on activation energy of the borides. This is different for the different boriding agents [33]. The saw-tooth morphology consisted of the iron borides that forms when carbon and other alloying elements are suppressed inlands from the surface of base alloy via the boron elements hence accumulation of the carbon and other elements in the diffusion region is higher than the base alloy. Namely, during the boriding process, the alloying elements in the composition of the alloy are redistributed. Meanwhile, the FeB and the Fe_2B layers have lower ability to dissolve the alloy elements such as carbon, silicon, so these alloy elements are pushed inlands via the boride layer during the boron diffusion. Therefore, as amount of the alloying elements increases, the boron diffusion in the alloy will become more difficult and resulting the saw-like boride structure will be denser and uniform [18,34].

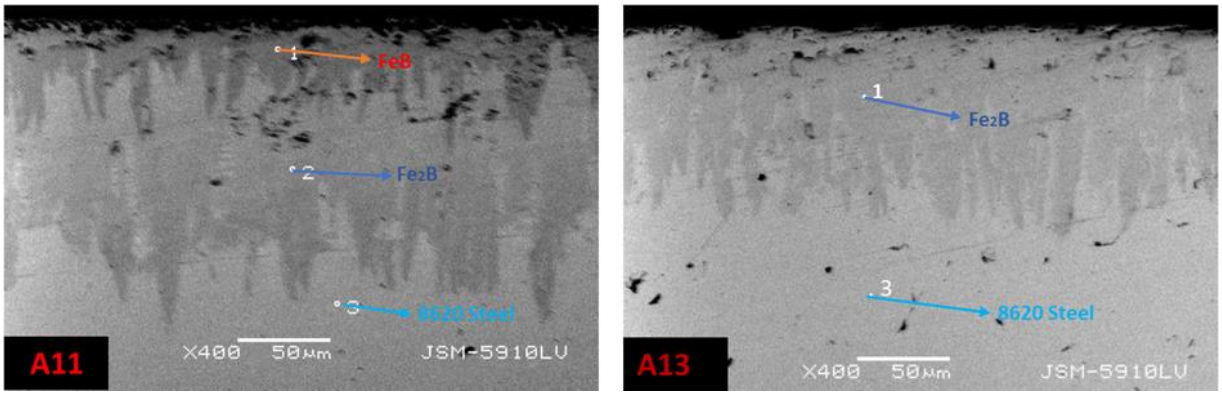


Fig. 2. SEM micrographs of some selected steels with the boride layer in the A11 and the A13 experiments

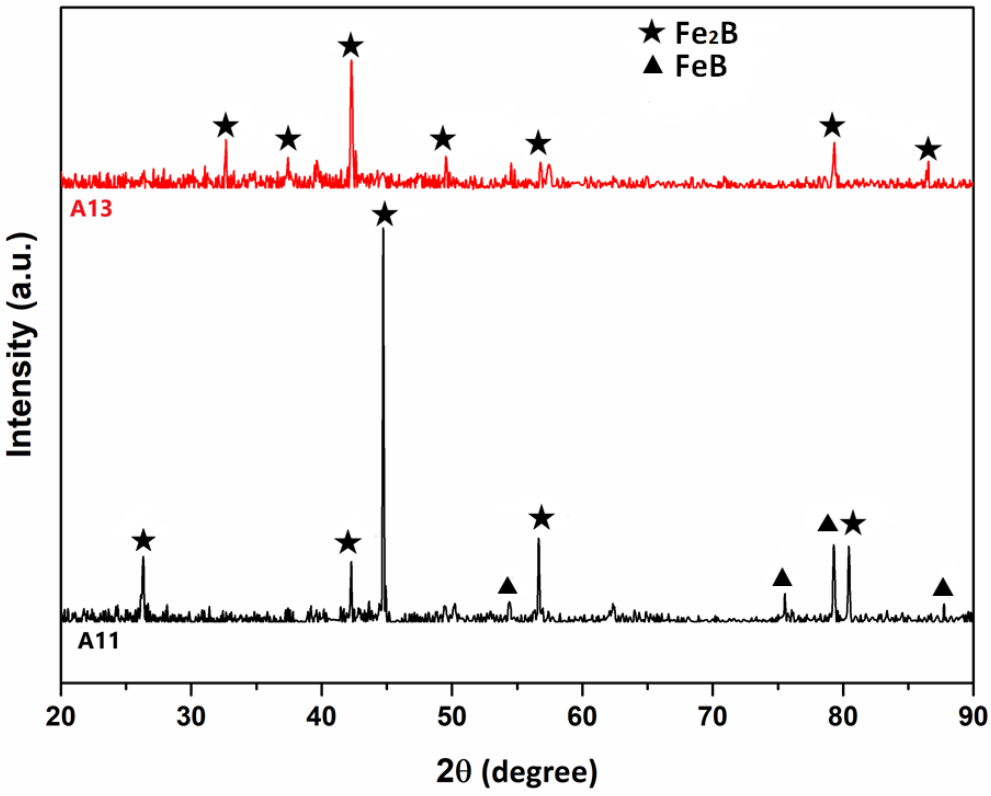


Fig. 3. XRD patterns of some selected steels with the boride layer in the A11 and the A13 experiments

Table 3. *EDS analysis of the steel with the boride layer in the A11 experiment from the surface to interior of the steel, wt. %*

	Si	Mn	P	S	Cr	Mo	Ni	B	C	Fe
Point 1	-	0.52	-	-	0.41	-	-	20.59	-	78.48
Point 2	-	0.67	-	-	0.48	-	-	6.15	-	92.7
Point 3	0.24	0.85	0.02	0.03	0.55	0.21	0.50	-	0.18	97.42

Furthermore, as it has been reported before that forming of the Fe_2B can be attributed to grain boundaries. The forming of the Fe_2B depends on full or deficient wetting of the grain boundary layers. If the wetting needed for the Fe_2B is provided, it affects mechanical behaviors [27].

CONCLUSİONS

Under predetermined experimental conditions, the solid boriding process with the chemical agents of the B_4C, the SiC and the KBF_4, and the liquid boriding process with the $Na_2B_4O_7$ and the B_4C provided the best hardness profiles for the boride layers achieved. Especially with the liquid boriding processes, the microstructures of the boride layers were found to be rather homogeneous. The most useful compositions for the solid and the liquid boriding processes were found to be 5% B_4C-90% SiC-5% KBF_4, and 70% $Na_2B_4O_7$ (borax)-30% B_4C, respectively for achieving the boride layer having optimal hardness and thickness on the AISI 8620 steel. Whereas, some bath compositions, especially 85% B_4C-15%Na_2CO_3 and 85% SiC-30% B_2O_3 for the solid boriding process and 70% borax-30% Al and 73% borax-24% SiC-3% NaCl for the liquid boriding process were found to be unsuitable respectively.

Acknowledgement

The report was funded by the Scientific and Technological Research Council of Turkey (TUBITAK) and the project number is 1139B411402992.

Conflicts of Interest

The authors declare that they have no competing financial interests or personal relationships that could have seem to influence the study reported in this paper.

REFERENCES

1. S. Roy, S. Sundararajan, The effect of heat treatment routes on the retained austenite and Tribomechanical properties of carburized AISI 8620 steel, Surf. Coat. Technol. 308 (2016) 236–243. https://doi.org/10.1016/j.surfcoat.2016.06.095.
2. E. Duru, F. Doğan, M. Uysal, H. Akbulut, S. Aslan, Fabrication and characterization of graphene oxide reinforced NiB composite coating by pulsed electrodeposition technique, Diam. Relat. Mater. 120 (2021) 108688. https://doi.org/10.1016/j.diamond.2021.108688.

3. S. Aslan, E. Duru, Microstructure and Wear Properties of Electrodeposited Ni-B-Al_2O_3 Composite Coating on Low Carbon Steel at Elevated Temperature, J. Mater. Eng. Perform. (2021). https://doi.org/10.1007/s11665-021-06290-2.
4. F. Doğan, E. Duru, M. Uysal, H. Akbulut, S. Aslan, Tribology Study of Pulse Electrodeposited Ni-B-SWCNT Composite Coating, JOM. 74 (2022) 574–583. https://doi.org/10.1007/s11837-021-05070-6.
5. Ş. Ürdem, E. Duru, H. Algül, M. Uysal, H. Akbulut, Evaluation of high temperature tribological behavior of electroless deposited NiB–Al_2O_3 coating, Wear. 482–483 (2021) 203960. https://doi.org/10.1016/j.wear.2021.203960.
6. G. Singh, P. Jasbir, S. Ratol, B.S. Bhullar, Investigate wear resistance of $TiAl_2O_3$ coating by detonation gun process on AISI 8620, Int. J. Emerg. Technol. 4 (2013) 123-131.
7. A. Motallebzadeh, E. Dilektasli, M. Baydogan, E. Atar, Evaluation of the effect of boride layer structure on the high temperature wear behavior of borided steels, Wear. 328–329 (2015) 110–114. https://doi.org/10.1016/j.wear.2015.01.029.
8. M.S. Gök, Y. Küçük, A. Erdoğan, M. Öge, E. Kanca, A. Günen, Dry sliding wear behavior of borided hot-work tool steel at elevated temperatures, Surf. Coatings Technol. 328 (2017) 54–62. https://doi.org/10.1016/j.surfcoat.2017.08.008.
9. T. Balusamy, T.S.N.S. Narayanan, K. Ravichandran, I. Song, M. Ho, Pack boronizing of AISI H11 tool steel : Role of surface mechanical attrition treatment, Vaccum. 97 (2013) 36–43. https://doi.org/10.1016/j.vacuum.2013.04.006.
10. E. Duru, F. Doğan, M. Uysal, H. Akbulut, S. Aslan, Optimization of Ni-B coating bath and effect of DMAB concentration on hardness and wear, Surf. Interfaces. 22 (2021) 100880. https://doi.org/10.1016/j.surfin.2020.100880.
11. A. Persson, J. Bergstrom, B. Christer, S. Hogmark, Thermal fatigue cracking of surface engineered hot work tool steels, Surf. Coat. Technol. 191 (2005) 216–227. https://doi.org/10.1016/j.surfcoat.2004.04.053.
12. A. Persson, S. Hogmark, J. Bergstrom, Influence of deposition temperature and time during PVD coating of CrN on corrosive wear in liquid aluminium, Surf. Coat. Technol. 147 (2001) 42–47. https://doi.org/https://doi.org/10.1016/S0257-8972(01)01366-4.
13. I. Gunes, S. Ulker, S. Taktak, Plasma paste boronizing of AISI 8620, 52100 and 440C steels, Mater. Des. 32 (2011) 2380–2386. https://doi.org/10.1016/j.matdes.2010.11.031.
14. B. Aktaş, M. Toprak, A. Çalık, A. Tekgüler, Effect of pack-boriding on the tribological behavior of Hardox 450 and HiTuf Steels, Rev. Adv. Mater. Sci. 59 (2020) 314–321.
15. M. Tabur, M. Izciler, F. Gul, I. Karacan, Abrasive wear behavior of boronized AISI 8620 steel, Wear. 266 (2009) 1106–1112. https://doi.org/10.1016/j.wear.2009.03.006.
16. C. Martini, G. Palombarini, G. Poli, D. Prandstraller, Sliding and abrasive wear behaviour of boride coatings, Wear. 256 (2004) 608–613. https://doi.org/10.1016/j.wear.2003.10.003.
17. M. Keddam, M. Kulka, Analysis of the growth kinetics of Fe2B layers by the integral method, J. Min. Metall. Sect. B Metall. 54 (2018) 361–367. https://doi.org/10.2298/JMMB180405026K.
18. C. Meric, S. Sahin, B. Backir, N.S. Koksal, Materials & Design Investigation of the boronizing effect on the abrasive wear behavior in cast irons, Mater. Des. 27 (2006) 751–757. https://doi.org/10.1016/j.matdes.2005.01.018.
19. Ş. Şen, İ. Özbek, U. Şen, C. Bindal, Mechanical behavior of borides formed on borided cold work tool steel, Surf. Coat. Technol. 135 (2001) 2–6. https://doi.org/https://doi.org/10.1016/S0257-8972(00)01064-1.
20. M. Kulka, N. Makuch, A. Pertek, A. Piasecki, An alternative method of gas boriding applied to

the formation of borocarburized layer, Mater. Charact. 72 (2012) 59–67. https://doi.org/10.1016/j.matchar.2012.07.009.

21. M. Kul, K.O. Oskay, A. Temizkan, B. Karaca, L.C. Kumruoğlu, B. Topçu, Effect of boronizing composition on boride layer of boronized GGG-60 ductile cast iron, Vacuum. 126 (2016) 80–83. https://doi.org/10.1016/j.vacuum.2016.01.021.

22. E.D.R. Cardenas, E. E. V, Lewis R, Perez, A. I. M, Ponce, J. L. B, Pinal, F. J. P, Dominguez, M. O, Arreola, Characterization and wear performance of boride phases over tool steel substrates, Adv. Mech. Eng. 8 (2016) 1–10. https://doi.org/10.1177/1687814016630257.

23. A. Günen, K.M. Döleker, M.E. Korkmaz, M.S. Gök, A. Erdogan, Characteristics, high temperature wear and oxidation behavior of boride layer grown on nimonic 80A Ni-based superalloy, Surf. Coat. Technol. 409 (2021). https://doi.org/10.1016/j.surfcoat.2021.126906.

24. R. Carrera-Espinoza, U. Figueroa-López, J. Martínez-Trinidad, I. Campos-Silva, E. Hernández-Sánchez, A. Motallebzadeh, Tribological behavior of borided AISI 1018 steel under linear reciprocating sliding conditions, Wear. 362–363 (2016) 1–7. https://doi.org/10.1016/j.wear.2016.05.003.

25. M. Kulka: Current Trends in Boriding. First Edit, Springer International Publishing, Poznan, 2019. https://doi.org/10.1007/978-3-030-06782-3.

26. O. Allaoui, N. Bouaouadja, G. Saindernan, Characterization of boronized layers on a XC38 steel, Surf. Coat. Technol. 201 (2006) 3475–3482. https://doi.org/10.1016/j.surfcoat.2006.07.238.

27. M. Kul, İ. Danacı, Ş. Gezer, B. Karaca, Effect of boronizing composition on hardness of boronized AISI 1045 steel, Mater. Lett. 279 (2020) 1–4. https://doi.org/10.1016/j.matlet.2020.128510.

28. A.A. Joshi, S.S. Hosmani, Pack-Boronizing of AISI 4140 Steel : Boronizing Mechanism and the Role of Container Design, Mater. Manuf. Process. 6914 (2014) 1062–1072. https://doi.org/10.1080/10426914.2014.921705.

29. I. Uslu, H. Comert, M. Ipek, O. Ozdemir, C. Bindal, Materials & Design Evaluation of borides formed on AISI P20 steel, Mater. Des. 28 (2007) 55–61. https://doi.org/10.1016/j.matdes.2005.06.013.

30. M. Keddam, M. Hudáková, J. Ptačinová, R. Moravčík, P. Gogola, Z. Gabalcová, P. Jurči, Characterization of boronized layers on Vanadis 6 tool steel, Surf. Eng. 34 (2021) 445–454. https://doi.org/10.1080/02670844.2020.1781377.

31. P. Jurči, M. Hudáková, Diffusion Boronizing of H11 Hot Work Tool Steel, J. Mater. Eng. Perform. 20 (2011) 1180–1187. https://doi.org/10.1007/s11665-010-9750-x.

32. A. Calik, A. Duzgun, A.E. Ekinci, S. Karakas, N. Ucar, Comparison of Hardness and Wear Behaviour of Boronized and Carburized AISI 8620 Steels, Acta Phys. Pol. A. 116 (2009) 1029–1032. https://doi.org/10.12693/aphyspola.116.1029.

33. M. Keddam, M. Hudáková, J. Ptačinová, M. Kusy, P. Jurči, Modelling of the Boronizing Kinetics of Vanadis 6 Steel by the Integral Diffusion Model, Prot. Met. Phys. Chem. Surf. 58 (2022) 347–355. https://doi.org/10.1134/S207020512202006X.

34. A. Yapici, S.E. Aydin, V. Koc, E. Kanca, M. Yildiz, Wear Behavior of Borided AISI D2 Steel under Linear Reciprocating Sliding Conditions, Prot. Met. Phys. Chem. Surf. 55 (2019) 341–351. https://doi.org/10.1134/S207020511902028X.